

The “horn” in the kaon-to-pion ratio

Jajati K. Nayak, Sarmistha Banik, and Jan-e Alam

Variable Energy Cyclotron Centre, 1/AF, Bidhan Nagar, Kolkata 700064, India

(Received 7 June 2010; published 30 August 2010)

A microscopic approach has been employed to study the kaon productions in heavy-ion collisions. The momentum-integrated Boltzmann equation has been used to study the evolution of strangeness in the system formed in heavy-ion collisions at relativistic energies. The kaon productions have been calculated for different center-of-mass energies ($\sqrt{s_{NN}}$) ranging from the Alternating Gradient Synchrotron (AGS) to the Relativistic Heavy Ion Collider (RHIC). The results have been compared with available experimental data. We obtain a nonmonotonic hornlike structure for K^+/π^+ when plotted with $\sqrt{s_{NN}}$ with the assumption of an initial partonic phase beyond a certain threshold in $\sqrt{s_{NN}}$. However, a monotonic rise of K^+/π^+ is observed when a hadronic initial state is assumed for all $\sqrt{s_{NN}}$. Experimental values of K^-/π^- are also reproduced within the ambit of the same formalism. Results from scenarios where the strange quarks and hadrons are formed in equilibrium and evolve with and without secondary productions have also been presented.

DOI: [10.1103/PhysRevC.82.024914](https://doi.org/10.1103/PhysRevC.82.024914)

PACS number(s): 25.75.Dw, 24.85.+p

I. INTRODUCTION

The lattice simulation of the quantum chromodynamic equation of state (EOS) predicts that the properties of nuclear matter at extreme densities and/or temperatures are governed by the partonic degrees of freedom [1–3]. A series of experiments have been performed [4] and planned [5] to produce such a partonic state of matter, called quark gluon plasma (QGP), by colliding nuclei at ultrarelativistic energies. Rigorous experimental and theoretical efforts are on to create and detect such a novel state of matter [6]. Various signals have been proposed for the detection of QGP—the pros and cons of these signals are matters of intense debate. The study of the ratio, $R^+ \equiv K^+/\pi^+$, is one such currently debated issue. R^+ is measured experimentally [7–10] as a function of the center-of-mass energy ($\sqrt{s_{NN}}$). It is observed that the R^+ increases with $\sqrt{s_{NN}}$ and then decreases beyond a certain value of $\sqrt{s_{NN}}$ giving rise to a hornlike structure, whereas the ratio $R^- \equiv K^-/\pi^-$ increases faster at lower $\sqrt{s_{NN}}$ and tends to saturate at higher $\sqrt{s_{NN}}$.

Explanation of this structure has ignited intense theoretical activities [11–19]. Several authors have attempted to reproduce the K^+/π^+ ratio using different approaches. While the authors in [12] use a hadronic kinetic model, in Ref. [13] high mass unknown hadronic resonances have been introduced through the Hagedorn formula to describe the data. In Ref. [14] a transition from a baryon-dominated system at low energy to a meson-dominated system at higher energy has been assumed to reproduce the ratio K^+/π^+ . The release of color degrees of freedom is assumed in [11] beyond a threshold in $\sqrt{s_{NN}}$ (resulting in large pion productions). The production of a larger number of pions than kaons from higher mass resonance decays has also been employed [16] to explain the data. In the present work we employ a microscopic model for the productions and evolution of strange quarks and hadrons depending on the collision energy. Here we examine whether the K^+/π^+ experimental data can differentiate between the following two initial conditions or two scenarios—after the collisions the system is formed in (I) the hadronic phase for all $\sqrt{s_{NN}}$ or (II)

the partonic phase beyond a certain threshold in $\sqrt{s_{NN}}$. Other possibilities, such as the formation of strangeness in complete thermal equilibrium and evolution in space-time (III) without and (IV) with secondary productions of quarks and hadrons, have been considered. (V) Results for an ideal case of zero strangeness in the initial state have also been presented.

In the context of strangeness enhancement as a signal of QGP formation, a similar approach [i.e., the assumption of an initial state where nonstrange sectors are in equilibrium but the strange degrees of freedom are out of equilibrium (having density much below their equilibrium values)] were considered in the 1980s. The strangeness production in a deconfined (partonic) phase is enhanced compared to their production in the confined (hadronic) phase primarily because even the lightest strange hadrons, the kaons, are much heavier than the strange quarks. Moreover, the strange quark has more degrees of freedom (six) in a deconfined matter compared to kaons. Therefore, the strangeness production during the space-time evolution of the system for a partonic initial state will be enhanced compared to the hadronic initial state, hence the enhanced production of strangeness could be an efficient signal for deconfinement [20–22]. In contrast to these studies, Gazdzicki and Gorenstein [11,23,24] considered, within the ambit of a statistical model, the strangeness production where both the strange and nonstrange degrees of freedom are in thermal equilibrium and the production of strangeness during the expansion stage is ignored. In the present work we would like to compare the results on the kaon-to-pion ratio from these two contrasting scenarios.

We assume that the nonstrange quarks and hadrons are in complete thermal (both kinetic and chemical) equilibrium and the strange quarks and strange hadrons are away from chemical equilibrium. Therefore, the evolution of the strange sector of the system is governed by the interactions between the equilibrium and nonequilibrium degrees of freedom. The momentum-integrated Boltzmann equation provides a possible framework for such studies. A similar approach has been used to study the sequential freeze-out of elementary particles in the early universe [25].

For the strangeness productions in the partonic phase we consider the processes of gluon fusion and light quarks annihilation. For the production of K^+ and K^- an exhaustive set of reactions involving thermal baryons and mesons have been considered. The time evolution of the densities are governed by the Boltzmann equation.

The paper is organized as follows. In Sec. II the rate of strangeness productions in the partonic and hadronic phases are discussed. The space-time evolution of the system is presented in Sec. III. Results are presented in Sec. IV and finally Sec. V is devoted to a summary and conclusions.

II. STRANGENESS PRODUCTIONS

The production of s and \bar{s} in the QGP and K^+ and K^- in the hadronic system are discussed below.

A. Strange quark productions in the QGP

The two main processes for the strange quark productions are gluon fusion ($gg \rightarrow s\bar{s}$) and quark (q)-antiquark (\bar{q}) annihilations ($q\bar{q} \rightarrow s\bar{s}$). The cross sections in the lowest-order QCD are given by [20]

$$\sigma_{q\bar{q} \rightarrow s\bar{s}} = \frac{8\pi\alpha_s^2}{27s} \left(1 + \frac{2m^2}{s}\right) w(s) \quad (1)$$

and

$$\sigma_{gg \rightarrow s\bar{s}} = \frac{2\pi\alpha_s^2}{3s} \left(G(s)\tanh^{-1}w(s) - \frac{7}{8} + \frac{31m^2}{8s}w(s) \right), \quad (2)$$

where m is the mass of the strange quark, $s = (p_1 + p_2)^2$ is the square of the center-of-mass energy of the colliding particles, p_i are the four-momenta of incoming particles, $G = 1 + 4m^2/s + m^4/s^2$, $w(s) = (1 - 4m^2/s)$, and α_s is the strong-coupling constant that depends on temperature [26].

B. K^+ and K^- productions in the hadronic system

The rate of $K^+(u\bar{s})$ and $K^-(\bar{u}s)$ productions in the hadronic phase can be categorized as due to (a) meson-meson (MM), (b) meson-baryon (MB), and (c) baryon-baryon (BB) interactions. In the present paper we quote only the main results for kaon productions in the hadronic matter and refer to [27] for details.

(a) For the first category $MM \rightarrow K\bar{K}$, we considered the following channels: $\pi\pi \rightarrow K\bar{K}$, $\rho\rho \rightarrow K\bar{K}$, $\pi\rho \rightarrow K\bar{K}^*$, and $\pi\rho \rightarrow K^*\bar{K}$. The invariant amplitude for these processes have been calculated from the following Lagrangians [27]. For the $K^*K\pi$ vertex the interaction is given by

$$\mathcal{L}_{K^*K\pi} = g_{K^*K\pi} K^{*\mu} \tau [K(\partial_\mu \pi) - (\partial_\mu K)\pi]. \quad (3)$$

Similarly for the $\rho K K$ vertex the interaction is

$$\mathcal{L}_{\rho K K} = g_{\rho K K} [K\tau(\partial_\mu K) - (\partial^\mu K)\tau K]\rho^\mu. \quad (4)$$

The isospin averaged cross section ($\bar{\sigma}$) for $MM \rightarrow K\bar{K}$ (i.e., $\pi\pi \rightarrow K\bar{K}$, $\rho\rho \rightarrow K\bar{K}$ and $\pi\rho \rightarrow K\bar{K}^*$, $\pi\rho \rightarrow K^*\bar{K}$) is

evaluated by using

$$\bar{\sigma} = \frac{1}{32\pi} \frac{P'}{sP} \int_{-1}^1 dx M(s, x), \quad (5)$$

where P and P' are the three-momenta of the meson and kaons in the center-of-mass frame, x is the cosine of the angle between P and P' . $M(s, x)$ is the isospin-averaged squared-invariant amplitude.

(b) For meson-baryon interactions the dominant channels are $\pi N \rightarrow \Lambda K$, $\rho N \rightarrow \Lambda K$, $\pi N \rightarrow N K \bar{K}$, and $\pi N \rightarrow N \pi K \bar{K}$. The isospin-averaged cross section is given by [28]

$$\bar{\sigma}_{MB \rightarrow YK} = \sum_i \frac{(2J_i + 1)}{(2S_1 + 1)(2S_2 + 1)} \frac{4\pi}{k_i^2} \times \frac{\frac{\Gamma_i^2}{4}}{(s^{\frac{1}{2}} - m_i)^2 + \Gamma_i^2/4} B_i^{\text{in}} B_i^{\text{out}}. \quad (6)$$

J_i , Γ_i , and m_i are the spin, width, and mass of the resonances, $(2S + 1)$ is the polarization states of the incident particles, and k is the center-of-mass momentum of the initial state. B^{in} and B^{out} are the branching ratios of initial- and final-state channels, respectively. The index i runs over all the resonance states. For interactions $\pi N \rightarrow \Lambda K$, $\rho N \rightarrow \Lambda K$ we have considered $N_1^*(1650)$, $N_2^*(1710)$, and $N_3^*(1720)$ as the intermediate states. Values of various hadronic masses and decay widths are taken from a particle data book [28].

(c) For the last category of reactions (i.e., for baryon-baryon interactions [29–31]) the dominant processes are $NN \rightarrow N \Lambda K$, $N \Delta \rightarrow N \Lambda K$, $\Delta \Delta \rightarrow N \Lambda K$, $NN \rightarrow NN K \bar{K}$, $NN \rightarrow NN \pi \pi K \bar{K}$, and $NN \rightarrow NN \pi K \bar{K}$.

The isospin-averaged cross section of kaon production from the process such as $N_1 N_2 \rightarrow N_3 \Lambda K$ is given by [29,30]

$$\bar{\sigma}_{NN \rightarrow N \Lambda K} = \frac{3m_N^2}{2\pi^2 p^2 s} \int_{W_{\text{min}}}^{W_{\text{max}}} dW W^2 k \int_{q_-^2}^{q_+^2} dq^2 \times \frac{f_{\pi NN}^2}{m_\pi^2} F^2(q^2) \frac{q^2}{(q^2 - m_\pi^2)^2} \bar{\sigma}_0(W; q^2). \quad (7)$$

The pion is the intermediate particle for the above interaction, m_N is the mass of N , W is the total energy in the center-of-mass system of the pion and N_2 , and $W_{\text{min}} = m_K + m_\Lambda$, $W_{\text{max}} = s^{1/2} - m_N$. $q_\pm^2 = 2m_N^2 - 2EE' \pm 2pp'$, where p, p' are the momenta and E, E' are the energies of N_1 and N_3 , respectively. We take $f_{\pi NN} = 1$ and to constrain the finite size of the interaction vertices we use the form factor $F = (\Lambda^2 - m_\pi^2)/(\Lambda^2 - q^2)$. $\bar{\sigma}_0$ is the isospin-averaged cross section of $\pi N_2 \rightarrow \Lambda K$. Cross sections for the processes $N \Delta \rightarrow N \Lambda K$ and $\Delta \Delta \rightarrow N \Lambda K$ have been taken from [30]. The cross section of other reactions (e.g., $NN \rightarrow NN K \bar{K}$, $NN \rightarrow NN \pi \pi K \bar{K}$, and $NN \rightarrow NN \pi K \bar{K}$) have been taken from [31]. In a baryon rich medium, K^- gets absorbed due to its interaction with the baryons. The reactions $K^- p \rightarrow \Lambda \pi^0$, $K^- p \rightarrow \sigma \pi^0$, $K^- n \rightarrow \sigma p$, $K^- p \rightarrow \bar{K}^0 n$, $K^- n \rightarrow K^- n$ have been considered for K^- absorption [31] in the nuclear matter.

C. Rate of strangeness productions

dN/d^4x ($\equiv R$), the number of s quarks produced per unit time per unit volume at temperature T and baryonic chemical potential μ_B is given by

$$\frac{dN}{d^4x} = \int \frac{d^3p_1}{(2\pi)^3} f(p_1) \int \frac{d^3p_2}{(2\pi)^3} f(p_2) v_{\text{rel}} \sigma, \quad (8)$$

where p_i 's are the momenta of the incoming particles and $f(p_i)$'s are the respective phase-space distribution functions (through which the dependence on T and μ_B is introduced), $v_{\text{rel}} = |v_1 - v_2|$ is the relative velocity of the incoming particles, and σ is the production cross sections for the reactions. The same equation can be used for kaon production by appropriate replacements of the phase-space factor and cross sections.

III. EVOLUTION OF STRANGENESS

The possibility of the formation of a fully equilibrated system in high-energy nuclear collisions is still a fiercely debated issue because of the finite size and lifetime of system. In the present work we assume that the strange quarks or the strange hadrons (depending on the value of $\sqrt{s_{NN}}$) produced as a result of the collisions are not in chemical equilibrium. The time evolution of the strangeness in either the QGP or the hadronic phase is governed by the momentum-integrated Boltzmann equation. We have assumed that the initial density of strange quarks or kaons (depending on the initial conditions I or II) is 20% away from the corresponding equilibrium density. We will comment on the amount of deviations from chemical equilibrium later.

A. Evolution in the QGP and hadronic phase

The momentum-integrated Boltzmann equation has been applied to study the freeze-out of elementary particles during the thermal expansion of the early universe [25]. In the present work we follow a similar procedure to study the evolution of the strange quarks and antiquarks in the QGP phase or kaons in the hadronic phase. The coupled equations describing the evolution of i (particle) and j (antiparticle) with proper time τ is given by

$$\begin{aligned} \frac{dn_i}{d\tau} &= R_i(\mu_B, T) \left(1 - \frac{n_i n_j}{n_i^{\text{eq}} n_j^{\text{eq}}} \right) - \frac{n_i}{\tau}, \\ \frac{dn_j}{d\tau} &= R_j(\mu_B, T) \left(1 - \frac{n_j n_i}{n_j^{\text{eq}} n_i^{\text{eq}}} \right) - \frac{n_j}{\tau}, \end{aligned} \quad (9)$$

where n_i (n_j) and n_i^{eq} (n_j^{eq}) are the nonequilibrium and equilibrium densities of the i (j) type of particles, respectively. R_i is the rate of production of particle i at temperature T and chemical potential μ_B , and τ is the proper time. The first term on the right-hand side of Eq. (9) is the production term and the second term represents the dilution of the system due to expansion. The variation of temperature and the baryonic chemical potential with time is governed by the hydrodynamic equations (next section). The indices i and j in Eq. (9) are

replaced by s, \bar{s} quark in the QGP phase and by K^+, K^- in the hadron phase, respectively.

B. Evolution in the mixed phase

For higher colliding energies (i.e., $\sqrt{s} \geq 8.76$ GeV) an initial partonic phase is assumed. The hadrons are formed at a transition temperature $T_c = 190$ MeV through a first-order phase transition from QGP to hadrons. The fraction of the QGP phase in the mixed phase at a proper time τ is given by [32,33]

$$f_Q(\tau) = \frac{1}{r-1} \left(r \frac{\tau_H}{\tau} - 1 \right), \quad (10)$$

where τ_Q (τ_H) is the time at which the QGP (mixed) phase ends, and r is the ratio of statistical degeneracy in QGP to the hadronic phase. The evolution of the kaons are governed by [32]

$$\begin{aligned} \frac{dn_{K^+}}{d\tau} &= R_{K^+}(\mu_B, T_c) \left(1 - \frac{n_{K^+} n_{K^-}}{n_{K^+}^{\text{eq}} n_{K^-}^{\text{eq}}} \right) - \frac{n_{K^+}}{\tau} \\ &\quad + \frac{1}{f_H} \frac{df_H}{d\tau} (\delta n_{\bar{s}} - n_{K^+}), \\ \frac{dn_{K^-}}{d\tau} &= R_{K^-}(\mu_B, T_c) \left(1 - \frac{n_{K^+} n_{K^-}}{n_{K^+}^{\text{eq}} n_{K^-}^{\text{eq}}} \right) - \frac{n_{K^-}}{\tau} \\ &\quad + \frac{1}{f_H} \frac{df_H}{d\tau} (\delta n_s - n_{K^-}). \end{aligned} \quad (11)$$

A similar equation exists for the evolution of s and \bar{s} quarks in the mixed phase (see [32] for details). In Eqs. (11) $f_H(\tau) = 1 - f_Q(\tau)$ represents the fraction of hadrons in the mixed phase at time τ . The last term stands for the hadronization of $\bar{s}(s)$ quarks to $K^+(K^-)$ [32,34]. Here δ is a parameter which indicates the fraction of $\bar{s}(s)$ quarks hadronizing to $K^+(K^-)$. $\delta = 0.5$ indicates the formation of K^+ and K^0 in the mixed phase because half of the \bar{s} form K^+ and the rest hadronize to K^0 .

C. Space-time evolution

The partonic/hadronic system produced in nuclear collisions evolves in space-time. The space-time evolution of the bulk matter is governed by the relativistic hydrodynamic equation

$$\partial_\mu T^{\mu\nu} = 0 \quad (12)$$

with boost invariance along the longitudinal direction [35]. In Eq. (12) $T^{\mu\nu} = (\epsilon + P)u^\mu u^\nu - g^{\mu\nu}P$ is the energy-momentum tensor for ideal fluid, ϵ is the energy density, P is the pressure, and u^μ is the hydrodynamic four-velocity. The net baryon number conservation in the system is governed by

$$\partial_\mu (n_B u^\mu) = 0, \quad (13)$$

where n_B is the net baryon density. Equations (12) and (13) have been solved (see [36,37] for details) to obtain the variation of temperature and baryon density with proper time. The initial temperatures corresponding to different $\sqrt{s_{NN}}$ are taken from Table I. The baryonic chemical potential at freeze-out is taken from the parametrization of μ_B with $\sqrt{s_{NN}}$ [38] (see also [16]) and the baryonic chemical potential at the initial

TABLE I. Initial conditions for the transport calculation. Colliding energies are in the center-of-mass frame.

$\sqrt{s_{NN}}$ (GeV)	T_i (GeV)	T_c (GeV)
3.32	0.115	—
3.83	0.128	—
4.8	0.150	—
6.27	0.160	—
7.6	0.187	—
8.76	0.210	0.190
12.3	0.225	0.190
17.3	0.25	0.190
62.4	0.3	0.190
130	0.35	0.190
200	0.40	0.190

state is obtained from the net baryon number conservation equation.

The initial temperatures of the systems formed after nuclear collisions have been evaluated from the measured hadronic multiplicity, dN/dy , by using the following relation:

$$T_i^3 = \frac{2\pi^4}{45\zeta(3)} \frac{1}{\pi R^2 \tau_i} \frac{90}{4\pi^2 g_{\text{eff}}} \frac{dN}{dy}, \quad (14)$$

where $\zeta(3)$ denotes the Riemann ζ function, R is the transverse radius [$\sim 1.1(N_{\text{part}}/2)^{1/3}$, N_{part} is the number of participant nucleons] of the colliding system, τ_i is the initial time, and g_{eff} is the statistical degeneracy. Initial temperatures for different $\sqrt{s_{NN}}$ are tabulated in Table I.

IV. RESULTS AND DISCUSSION

The variation of the number of strange antiquarks produced per unit volume per unit time with temperature has been displayed in Fig. 1 for a baryonic chemical potential $\mu_q = 107$ MeV. It is observed that the process of gluon fusion dominates over the $q\bar{q}$ annihilation for the entire temperature range under consideration, primarily because at high $\mu_B (= 3\mu_q)$ the number of antiquarks is suppressed. In Fig. 2, the production rate of K^+ from the $MM \rightarrow K\bar{K}$ type of reactions

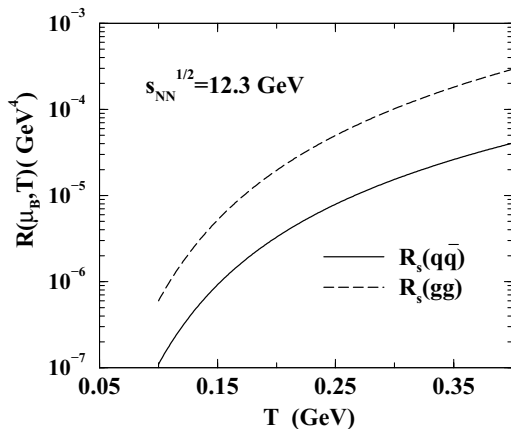
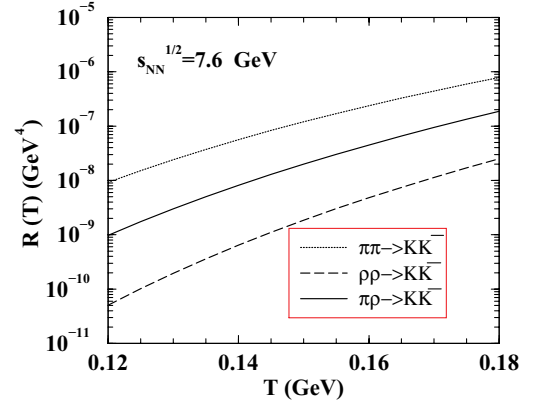

 FIG. 1. Rate of production of \bar{s} quark from $gg \rightarrow s\bar{s}$ and $q\bar{q} \rightarrow s\bar{s}$ with temperature.


FIG. 2. (Color online) The rate of kaon production from dominant meson-meson interactions with temperature.

has been depicted for $\sqrt{s_{NN}} = 7.6$ GeV. The production rate from pion annihilation dominates over the reactions that involves ρ mesons, because the thermal phase-space factor of ρ is small due its larger mass compared to pions and smaller production cross section. Results for interactions involving mesons and baryons are displayed in Fig. 3. It is observed that the interactions involving pions and nucleons in the initial channels dominate over that which has a ρ meson in the incident channel. In fact, contributions from the reactions $\rho N \rightarrow \Lambda K$ has a negligible effect on the total production from the meson-baryon interactions. The kaon production from baryon-baryon interactions is displayed in Fig. 4. The contributions from $N\Delta \rightarrow N\Lambda K$ dominates over the contributions from $NN \rightarrow N\Lambda K$ and $\Delta\Delta \rightarrow N\Delta K$ for the temperature range $T = 120$ to 180 MeV.

In Fig. 5 the rates of K^+ productions from meson-meson interactions has been compared with those involving baryons [i.e., with meson-baryon and baryon-baryon interactions for different $\sqrt{s_{NN}}$ (different μ_B)]. The results clearly indicate the dominant role of baryons at lower collision energies which diminishes with increasing $\sqrt{s_{NN}}$. At low temperature the baryonic contribution is more than the mesonic one for lower beam energy. The rate of productions (from MB + BB interactions) at $\sqrt{s_{NN}} = 4.8$ GeV is more compared to the rates

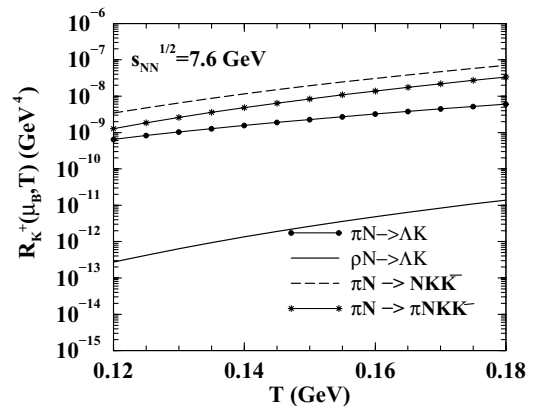


FIG. 3. Rate of kaon productions from the meson-baryon interactions with temperature.

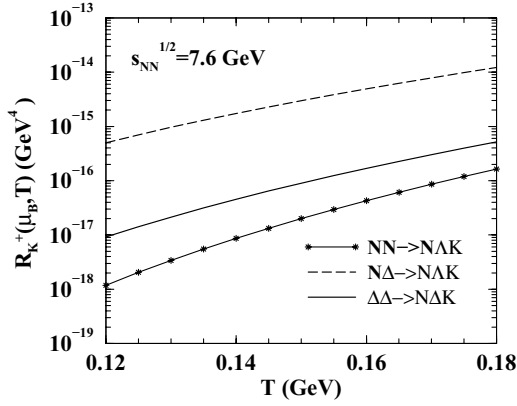


FIG. 4. Rate of kaon productions from baryon-baryon interactions with temperature.

at $\sqrt{s_{NN}} = 7.6$ and 200 GeV, since μ_B at $\sqrt{s_{NN}} = 4.8$ GeV is more (see Table II). The production rate from pure mesonic interactions does not depend on μ_B hence the same for all. It is quite clear from the results displayed in Fig. 5 that the greater the baryonic chemical potential (the lower the center-of-mass energy), the greater is the rate from BB and MB interactions compared to MM interactions. For a system having a lower chemical potential (a higher center-of-mass energy) the rate of production from mesonic interactions is dominant.

A comparison is made between rates of kaon productions from meson-meson (MM) and meson-baryon (MB) plus baryon-baryon (BB) interactions for $\sqrt{s_{NN}} = 7.6$ GeV. At this energy baryons and mesons are equally important as shown in Fig. 6.

In Fig. 7 the net rates of productions for K^+ and K^- have been depicted for $\sqrt{s_{NN}} = 7.6$ GeV (left panel) and 200 GeV (right panel). At $\sqrt{s_{NN}} = 7.6$ GeV the production of K^+ dominates over K^- for the entire temperature range. However, for large $\sqrt{s_{NN}}$ (low μ_B) the productions of K^+ and K^- are similar. The strong absorption of the K^- by nucleons in a baryon-rich medium results in a lower production yield of K^- compared to K^+ . This may be contrasted with the experimental findings of the BRAHMS experiment [9] where it is observed that at mid rapidity [small μ_B due to nuclear transparency at

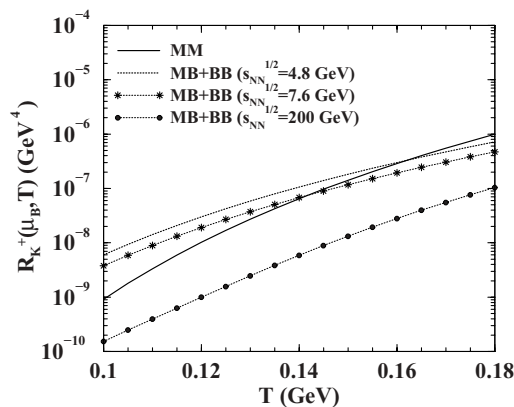


FIG. 5. Rate of kaon productions from meson-meson (MM) interactions, meson-baryon (MB), and baryon-baryon (BB) interactions at different center-of-mass energies.

TABLE II. Chemical potential for different center-of-mass energies.

Center-of-mass energy ($\sqrt{s_{NN}}$) (in GeV)	Chemical potential (μ_B) (MeV)
3.32	595
3.83	568
4.8	542
6.27	478
7.6	432
8.76	398
12.3	321
17.3	253
62.4	86
130	43
200	28

Relativistic Heavy Ion Collider (RHIC) energy] the K^+ and K^- yields are similar but at large rapidity (large μ_B) the K^- yield is smaller than K^+ due to large K^- nucleon absorption.

In Fig. 8 the variations of R^+ with $\sqrt{s_{NN}}$ are depicted. The experimental data on R^+ is well reproduced if a partonic initial phase (scenario II) is assumed beyond $\sqrt{s_{NN}} = 8.7$ GeV. A ‘‘mindless’’ extrapolation of the hadronic initial state (scenario I) for all the $\sqrt{s_{NN}}$ up to the RHIC energy show an increasing trend in disagreement with the experimental data at higher $\sqrt{s_{NN}}$. In both the scenarios I and II the curves at higher $\sqrt{s_{NN}}$ (RHIC energies) become flatter. That is because at higher energies the K^+ productions in the hadronic phase are dominated by mesonic interactions and the production rates from mesons are the same for all $\sqrt{s_{NN}}$ for a given temperature range. But at lower energies the rates of kaon productions are dominated by the effective interactions among the baryonic degrees of freedom. The composition of matter formed in heavy-ion collision changes from a matter dominated by baryons to a matter dominated by mesons with the increase in colliding energy. The μ_B changes from 86 MeV to 28 MeV as $\sqrt{s_{NN}}$ varies from 62.4 GeV to 200 GeV (Table II). The change in the K^+ production in the hadronic phase due to the change in μ_B previously mentioned is marginal—resulting in the flatness in R^+ at higher energies. The decrease of the value of the

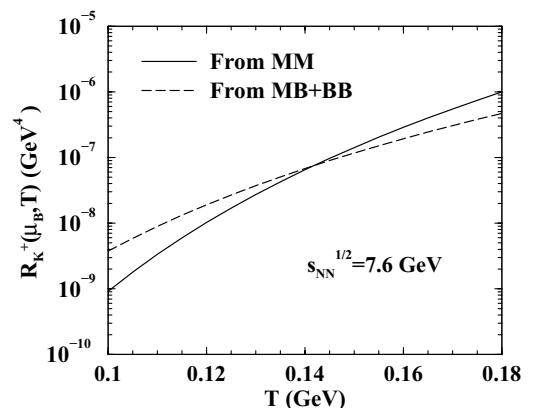


FIG. 6. Comparison between rates of kaon productions from MM and MM + MB interactions with temperature.

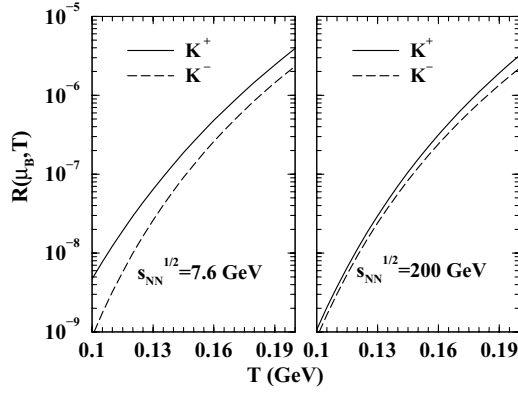


FIG. 7. Total K^+ and K^- production rates with temperature at center-of-mass energy equal to 7.6 GeV and 200 GeV.

R^+ beyond $\sqrt{s_{NN}} = 7.6$ GeV showing “hornlike” structure happens only when an initial partonic phase is considered. Such a nonmonotonic behavior of R^+ can be understood as due to larger entropy productions from the release of large color degrees of freedom (resulting in more pions yield) compared to strangeness beyond energy 7.6 GeV.

In Fig. 9, the variations of R^- with $\sqrt{s_{NN}}$ is displayed. R^- has a lower value compared to R^+ at lower energies since K^- get absorbed in the baryonic medium. At higher energies K^- is closer to K^+ because the production of K^+ and K^- is similar in a baryon-free medium, which may be realized at higher collision energies.

In Fig. 10 the R^+ is depicted as a function of $\sqrt{s_{NN}}$ for other scenarios (III, IV, and V). On the one hand, when the strange quarks and kaons are formed in complete equilibrium but their secondary productions are neglected during the evolution (scenario III) then the data is well reproduced. On the other hand, in scenario IV when the system is formed in equilibrium (as in scenario III) but the productions of strange quarks and kaons are switched on through secondary processes then the

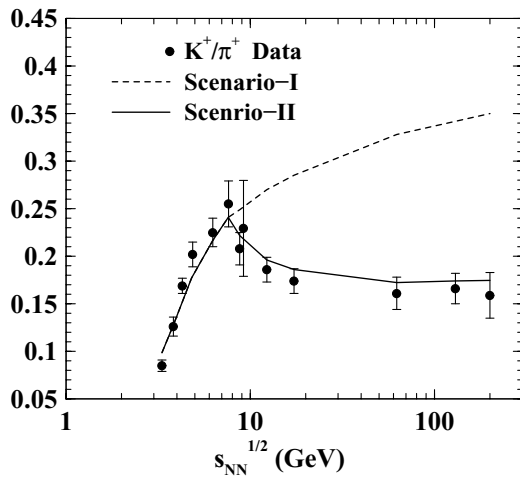


FIG. 8. K^+/π^+ ratio for different center-of-mass energies. Scenario I represents the pure initial hadronic scenario for all center-of-mass energies. Scenario II represents the calculation with hadronic initial conditions for low $\sqrt{s_{NN}}$ and partonic initial conditions for higher $\sqrt{s_{NN}}$. See the text for details.

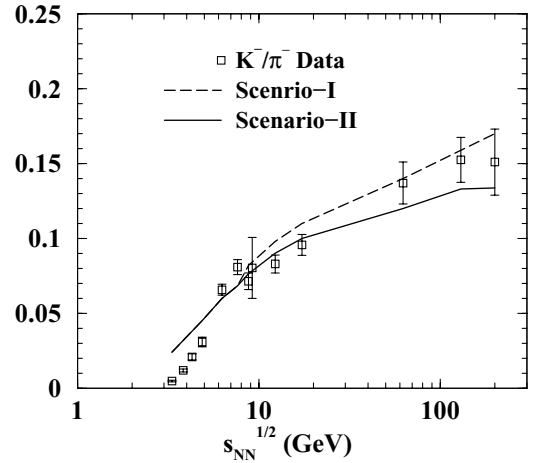


FIG. 9. K^-/π^- ratio for different center-of-mass energies. Scenario I represents the pure initial hadronic scenario for all center-of-mass energies. Scenario II represents the calculation with hadronic initial conditions for low $\sqrt{s_{NN}}$ and partonic initial conditions for higher $\sqrt{s_{NN}}$. See the text for details.

data is slightly overestimated at high $\sqrt{s_{NN}}$. However, we have seen that the data are also reproduced well in scenario II as discussed. This indicates that the deficiency of strangeness below its equilibrium value as considered in scenario II is compensated by the secondary productions. In scenario V we assumed that vanishing initial strangeness and observed that the production of strangeness throughout the evolution is not sufficient to reproduce the data. The productions from secondary processes are small but not entirely negligible (scenario V). In Fig. 11 the R^- has been displayed as a function of $\sqrt{s_{NN}}$. A trend similar to the results shown in Fig. 10 is observed. The data are overestimated for the intermediate $\sqrt{s_{NN}}$ in scenario IV, reproduced well in scenario III, and underestimated for scenario V.

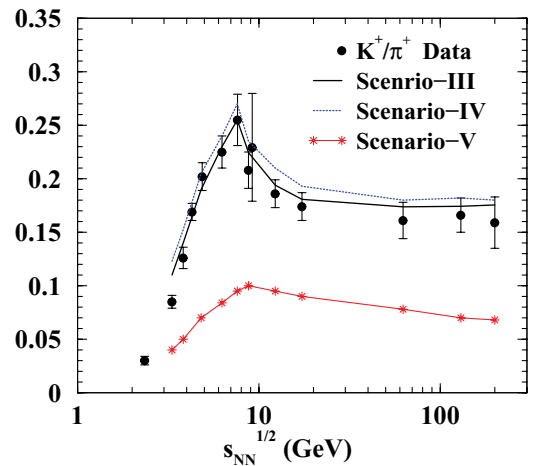


FIG. 10. (Color online) K^+/π^+ ratio for different center-of-mass energies. Scenario III assumes complete equilibrium of strange quarks and hadrons. The production through secondary processes have been ignored. Scenario IV is the same as scenario III with secondary productions processes on and scenario V represents zero strangeness initially but secondary productions are switched on.

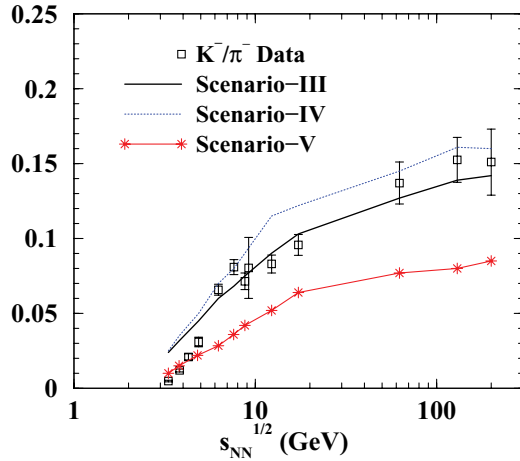


FIG. 11. (Color online) Same as Fig. 10 for K^-/π^- .

V. SUMMARY AND CONCLUSIONS

The evolution of the strangeness in the system formed in nuclear collisions at relativistic energies have been studied within the framework of a momentum-integrated Boltzmann equation. The Boltzmann equation has been used to study the evolution of s and \bar{s} in the partonic phase and K^- and K^+ in the hadronic phase. The calculation has been done for different center-of-mass energies ranging from AGS to RHIC. We get a nonmonotonic variation of K^+/π^+ with $\sqrt{s_{NN}}$ when

an initial partonic phase is assumed for $\sqrt{s_{NN}} = 8.76$ GeV and beyond. A monotonic rise of K^+/π^+ is observed when a pure hadronic scenario is assumed for all center-of-mass energies. The K^-/π^- data are unable to differentiate between the two initial conditions mentioned before.

Some comments on the values of the initial parameter are in order at this point. We have seen that a 10% variation in the initial temperature does not change the results drastically. We have assumed that the initial density of strange quarks or kaons, depending on the scenario I or II, is about 20% away from the corresponding equilibrium density. For results from a scenario where strange quarks or kaons are formed in complete equilibrium and the production is ignored during the evolution then the data is well reproduced (scenario III). If the the strangeness is produced in equilibrium and the production is included during the expansion stage then the data are overestimated. However, if the system is formed with zero strangeness then the theoretical results underestimate the data substantially. This indicates that the production of strangeness during the expansion of the system is small but not entirely negligible. The deficiency assumed in scenario II is compensated by the production during evolution.

ACKNOWLEDGMENTS

J. A. and S. B. are supported by DAE-BRNS project Sanction No. 2005/21/5-BRNS/2455. We thank B. Mohanty and Lokesh Kumar for providing the experimental data.

-
- [1] F. Karsch, *Prog. Part. Nucl. Phys.* **62**, 503 (2009).
 [2] D. E. Miller, *Phys. Rep.* **443**, 55 (2007).
 [3] Z. Fodor and S. Katz, *J. High Energy Phys.* **04** (2004) 050.
 [4] I. Arsene *et al.* (BRAHMS Collaboration), *Nucl. Phys. A* **757**, 1 (2005); B. B. Back *et al.* (PHOBOS Collaboration), *ibid.* **757**, 28 (2005); J. Adams *et al.* (STAR Collaboration), *ibid.* **757**, 102 (2005); K. Adcox *et al.* (PHENIX Collaboration), *ibid.* **757**, 184 (2005).
 [5] C. W. Fabjan (ALICE Collaboration), *J. Phys. G* **35**, 104038 (2008); D. d’Enterria (CMS Collaboration), *ibid.* **35**, 104039 (2008); N. Grau (ATLAS Collaboration), *ibid.* **35**, 104040 (2008).
 [6] *Quark Matter 2008—The 20th International Conference on Ultrarelativistic Nucleus-Nucleus Collisions, Jaipur, India, 2008*, edited by J. Alam, S. Chattopadhyay, T. Nayak, B. Sinha, and Y. P. Vijoyi [*J. Phys. G* **35** (2008)]; *Quark Matter 2009—The 21st International Conference on Ultrarelativistic Nucleus-Nucleus Collisions, Knoxville, TN, 2009*, edited by P. Stankus, D. Silvermyr, S. Sorensen, and V. Greene [*Nucl. Phys. A* **830** (2009)].
 [7] C. Alt *et al.* (NA49 Collaborations), *Phys. Rev. C* **77**, 024903 (2008).
 [8] B. I. Abelev *et al.* (STAR Collaboration), *Phys. Rev. C* **81**, 024911 (2010).
 [9] I. G. Bearden *et al.* (BRAHMS Collaboration), *Phys. Rev. Lett.* **94** 162301 (2005).
 [10] S. V. Afanasiev *et al.* (NA49 Collaboration), *Phys. Rev. C* **66**, 054902 (2002).
 [11] M. Gazdzicki and M. Gorenstein, *Acta Phys. Pol. B* **30**, 2705 (1999).
 [12] B. Tomasik and E. E. Kolomeitsev, *Eur. Phys. J. C* **49**, 115 (2007); B. Tomasik, [arXiv:nucl-th/0509101](https://arxiv.org/abs/nucl-th/0509101).
 [13] S. Chatterjee, R. M. Godbole, and Sourendu Gupta, *Phys. Rev. C* **81**, 044907 (2010).
 [14] J. Cleymans, H. Oeschler, K. Redlich, and S. Wheaton, *Eur. Phys. J. A* **29**, 119 (2006).
 [15] M. Gazdzicki, *J. Phys. G* **30**, S701 (2004).
 [16] A. Andronic, P. Braun-Munzinger, and J. Stachel, *Nucl. Phys. A* **772**, 167 (2006); **678**, 516(E) (2009).
 [17] J. K. Nayak, J. Alam, B. Mohanty, P. Roy, and A. K. Dutt-Mazumder, *Acta Phys. Slov.* **56**, 27 (2006).
 [18] J. Letessier and J. Rafelski, *Eur. Phys. J. A* **35**, 221 (2008).
 [19] A. Tawfik, *Fizika B* **18**, 141 (2009).
 [20] J. Rafelski and B. Muller, *Phys. Rev. Lett.* **48**, 1066 (1982).
 [21] P. Koch, B. Müller, and J. Rafelski, *Phys. Rep.* **142**, 167 (1986).
 [22] J. Rafelski and J. Letessier, *Acta Phys. Pol. B* **30**, 3559 (1999).
 [23] M. Gazdzicki, *Acta Phys. Pol. B* **35**, 187 (2004).
 [24] M. Gorenstein, *J. Phys. G* **28**, 1623 (2002).
 [25] E. Kolb and M. S. Turner, *Early Universe* (Westview, Boulder, CO, 1994).
 [26] O. Kaczmarek and F. Zantow, *Phys. Rev. D* **71**, 114510 (2005).
 [27] G. E. Brown *et al.*, *Phys. Rev. C* **43**, 1881 (1991).
 [28] C. Amslar *et al.*, *Phys. Lett. B* **667**, 1 (2008).
 [29] J. Q. Wu and C. M. Ko, *Nucl. Phys. A* **499**, 810 (1989).
 [30] J. Randrup and C. M. Ko, *Nucl. Phys. A* **343**, 519 (1980); **411**, 537 (1983).

- [31] G. Q. Li, C. H. Lee, and G. E. Brown, *Nucl. Phys. A* **625**, 372 (1997).
- [32] J. Kapusta and A. Mekjian, *Phys. Rev. D* **33**, 1304 (1986).
- [33] J. Alam, S. Raha, and B. Sinha, *Phys. Rep.* **273**, 243 (1996).
- [34] T. Matsui, B. Svetitsky, and L. D. McLerran, *Phys. Rev. D* **34**, 783 (1986); **34**, 2047 (1986).
- [35] J. D. Bjorken, *Phys. Rev. D* **27**, 140 (1983).
- [36] T. S. Biró, E. van Doorn, B. Müller, M. H. Thoma, and X. N. Wang, *Phys. Rev. C* **48**, 1275 (1993).
- [37] J. Alam, P. Roy, S. Sarkar, S. Raha, and B. Sinha, *Int. J. Mod. Phys. A* **12**, 5151 (1997).
- [38] O. Ristea (BRAHMS Collaboration), *Rom. Rep. Phys.* **56**, 659 (2004).